Available online at www.pelagiaresearchlibrary.com

Pelagia Research Library

Pelagia Research Library

Advances in Applied Science Research, 2015, 6(1):49-58

Pelagia Research Library

ISSN: 0976-8610
CODEN (USA): AASRFC

Unsteady slip flow of blood through constricted artery

Manish Gaur and Manoj Kumar Gupta

Department of Mathematics, Government College, Kota, Rajasthan, India

---

ABSTRACT

Considering the Casson fluid as blood; the unsteady flow through a constricted artery has been studied. The governing equations have been solved by using the perturbation technique. Expressions for axial velocity, shear Stress, volumetric flow rate and plug flow velocity are obtained. The results are shown and discussed through graphs; choosing suitable parameters. The study shows that the axial velocity, wall shear stress and the volumetric flow rate decrease when the time increases along the axial distance. The axial velocity and the volumetric flow rate rise with an increase in slip velocity. The non – plug flow velocity, volumetric flow rate and wall shear stress decrease but the plug flow velocity increases with increase in stenosis height along axial distance.

Keywords: Casson Fluid; Constricted Artery; Slip Boundary Condition; Yield Stress.

INTRODUCTION

The hemodynamic behaviour of flows through the constricted arteries have always drawn attention of the researchers as it puts the health at risk which proves sometimes fatal. One basic reason of the constriction of the artery is the deposit of some fatty and fibrous tissues in the arterial wall which restricts the normal blood flow through the artery. Many research workers have made valuable contributions to understand the various flow properties through the constricted arteries.

A.C. Burton [1] made several experiments to study the effects of whole body accelerations on human bodies and presented empirical data regarding the relations between blood flows and the radii of the blood vessels. D.F. Young [2] discussed the effect of an axially symmetric time-dependent stenotic growth into the lumen of a tube of constant cross-section over the steady flow of a Newtonian fluid. P. Chaturani et al. [3] studied the pulsatile flow of a Casson fluid through stenosed arteries with application to blood flow. S. Chakravarty et al. [4] presented a mathematical model for the blood flow through an overlapping time-dependent arterial stenosis by taking the experimentally established viscoelastic properties of the blood and deformability of the arterial wall. A.V. Mernone [5] et al. performed a mathematical study of peristaltic transport of a Casson fluid and found the analytical and numerical solutions for the zeroth and first order in stream function. H. Jung et al. [6] studied the asymmetric flows of non – Newtonian fluids in symmetric stenosed artery and discussed the characteristics of pulsatile blood flow. R.N. Pralhad et al. [7] modelled the arterial stenosis and studied its application in blood diseases assuming blood as a couple – stress fluid. K.Y. Volokh [8] studied the stresses in growing soft tissues and showed that the uniform volumetric growth can lead to the deposits of residual stresses in blood arteries due to the material anisotropy. T. Ishikawa [9] performed the numerical simulation of a low- hematocrit blood flow in a small artery with stenosis and showed that the erythrocytes are considerably deformed around the stenosis. S.U. Siddiqui et al. [10] studied pulsatile flow of blood through stenosed arteries and found that the width of the plug core region increases with increasing value of yield stress at any time. Gaur and Gupta. [11] presented a Casson fluid model for the steady flow

through a stenosed blood vessel in which the authors showed that the axial velocity, volumetric flow rate and pressure gradient increase with the increase in slip velocity and decrease with growth in yield stress. Gaur and Gupta [12] studied the slip effects on steady flow through a stenosed blood artery and showed that axial velocity, volumetric flow rate and pressure gradient decrease along the radial distance as the slip length increases but the wall shear stress increases with increase in slip length. Gaur and Gupta [13] discussed the steady blood flow under magnetic effects through an axially symmetric stenosed artery and found that increments in magnetic field gradients and slip velocity increase the axial velocity and flow flux. Gaur and Gupta [14] studied the porous effects on blood flow through a stenosed artery under slip conditions and found that the permeability of the arterial wall increases the axial velocity, plug flow velocity, flow flux and pressure gradient along axial and radial distances.

2. Mathematical Formulation

Let us consider an incompressible blood with a laminar unsteady flow through a cylindrical blood artery which is stenosed with an axially symmetric stenosis. The geometrical diagram of the stenosis is given below:

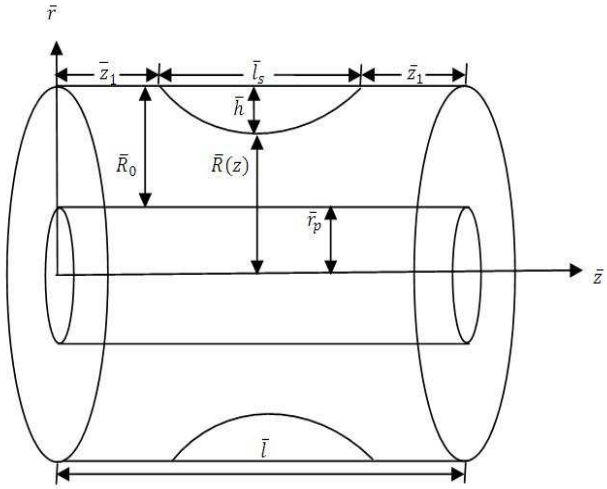

Let $\bar{R}(\bar{z})$ be the radius of the vessel in the constricted region and $\bar{R}_0$ in the non – stenotic area given as [2]:

$$\bar{R}(\bar{z}) = \begin{cases} \bar{R}_0 - \frac{\bar{h}}{2}\left[1 + \cos\frac{2\pi}{\bar{l}_s}\left(\bar{z}_1 + \bar{l}_s - \bar{z}\right)\right]; & \bar{z}_1 \le \bar{z} \le \bar{z}_1 + \bar{l}_s \\ \bar{R}_0 & ; \text{ otherwise} \end{cases} \quad (2.1)$$

where $\bar{h}, \bar{l}_s$ and $\bar{z}_1$ are the maximum height, length and the location of the stenosis in the vessel of the length $\bar{l}$. Also, let $\bar{r}$ and $\bar{z}$ represent the radial and axial coordinates.

Here the blood is assumed to behave like a Casson fluid.

Considering the above assumptions, the equations of motion for the blood can be written as

$$\bar{\rho}\frac{\partial \bar{v}_c}{\partial \bar{t}} = -\frac{\partial \bar{p}}{\partial \bar{z}} + \frac{1}{\bar{r}}\frac{\partial}{\partial \bar{r}}(\bar{r}\bar{\tau}_c) \quad (2.2)$$

$$\frac{\partial \bar{p}}{\partial \bar{r}} = 0 \quad (2.3)$$

Where $\bar{\rho}$ denotes the density of blood, $\bar{p}$ is the pressure at any point at time $\bar{t}$ and $\bar{\tau}_c$ is the shear stress. The constitutive equations for Casson fluid are:

$$F(\bar{\tau}_c) = -\frac{\partial \bar{v}_c}{\partial \bar{r}} = \frac{1}{\bar{k}_c}\left(\bar{\tau}_c^{1/2} - \bar{\tau}_y^{1/2}\right)^2 \text{ for } \bar{\tau}_c \ge \bar{\tau}_y \quad (2.4)$$

$$\frac{\partial \bar{v}_c}{\partial \bar{r}} = 0 \qquad \text{for } \bar{\tau}_c \le \bar{\tau}_y \quad (2.5)$$

Here $\bar{v}_c$ gives the axial velocity of blood, $\bar{\tau}_y$ represents the yield stress and $\bar{k}_c$ is the fluid viscosity. The equations (2.2) to (2.5) are governed with the following boundary conditions:

$$\left.\begin{aligned} \bar{v}_c &= \bar{v}_s \quad \text{at } \bar{r} = \bar{R}(\bar{z}) \\ \bar{\tau}_c &= \text{Finite value} \quad \text{at } \bar{r} = 0 \end{aligned}\right\} \tag{2.6}$$

where $\bar{v}_s$ is the slip velocity in the axial direction.

As the pressure gradient is a function of $\bar{z}$ and $\bar{t}$, its form can be taken from [1] as

$$\frac{\partial \bar{p}}{\partial \bar{z}}(\bar{z}, \bar{t}) = \bar{p}_0(\bar{z}) + \bar{p}_1(\bar{z}) \cos(\bar{\omega}.\bar{t}) \tag{2.7}$$

Here $\bar{p}_0$ is the steady – state amplitude and $\bar{p}_1$ is the fluctuating amplitude of the pressure gradient with a period $\bar{\omega} = 2\pi\bar{f}$ where $\bar{f}$ is the pulse frequency.

Applying the following non – dimensional quantities:

$$R(z) = \frac{\bar{R}(\bar{z})}{\bar{R}_0},\ z = \frac{\bar{z}_1 + \bar{l}_s - \bar{z}}{\bar{l}_s},\ r = \frac{\bar{r}}{\bar{R}_0},\ \tau_c = \frac{\bar{\tau}_c}{\bar{p}_0 \bar{R}_0/2},\ \tau_y = \frac{\bar{\tau}_y}{\bar{p}_0 \bar{R}_0/2},\ v_c = \frac{\bar{v}_c}{\bar{p}_0 \bar{R}_0^2/2\bar{k}_c},\ v_s = \frac{\bar{v}_s}{\bar{p}_0 \bar{R}_0^2/2\bar{k}_c},$$

$$H = \frac{\bar{h}}{\bar{R}_0},\ \alpha^2 = \frac{\bar{\omega}\bar{\rho}\bar{R}_0^2}{\bar{k}_c},\ t = \bar{\omega}.\bar{t},\ e = \frac{\bar{p}_1}{\bar{p}_0} \tag{2.8}$$

where e represents the amplitude of the flow and α defines the pulsatile Reynold number which is also known as the Womersley parameter.

Hence the dimensionless radius of the stenotic area of the artery is

$$R(z) = \begin{cases} 1 - H\cos^2 \pi z\,; & 0 \le z \le 1 \\ 1 \quad\quad\quad\quad ; & \text{otherwise} \end{cases} \tag{2.9}$$

The non – dimensional form of equation of the motion (2.2) is

$$\alpha^2 \frac{\partial v_c}{\partial t} = -2\varphi + \frac{1}{r}\frac{\partial}{\partial r}(r\tau_c) \tag{2.10}$$

Where $\varphi \equiv \varphi(t) = 1 + e\cos t$

The non – dimensional constitutive equations of Casson fluid are

$$-\frac{\partial v_c}{\partial r} = (\tau_c^{1/2} - \tau_y^{1/2})^2 \quad \text{for } \tau_c \ge \tau_y \tag{2.11}$$

$$\frac{\partial v_c}{\partial r} = 0 \quad \text{for } \tau_c \le \tau_y \tag{2.12}$$

The dimensionless boundary conditions are

$$\left.\begin{aligned} v_c &= v_s \quad \text{at } r = R(z) \\ \tau_c &= \text{Finite value} \quad \text{at } r = 0 \end{aligned}\right\} \tag{2.13}$$

3. Method of Solution

In order to get the required solutions of the problem, the perturbation method is used for which $\alpha^2 << 1$ is taken to maintain the non – Newtonian nature of the blood in which a plug flow region is developed through the constricted arteries in small blood vessels like coronary arteries. Then the axial velocity v_c, plug flow velocity v_p, shear stress τ_c and the plug core radius r_p can be expressed in the powers of α^2 given as

$$v_c = v_{c0} + \alpha^2 v_{c1} + \alpha^4 v_{c2} + \cdots \tag{3.1}$$
$$v_p = v_{p0} + \alpha^2 v_{p1} + \alpha^4 v_{p2} + \cdots \tag{3.2}$$
$$\tau_c = \tau_{c0} + \alpha^2 \tau_{c1} + \alpha^4 \tau_{c2} + \cdots \tag{3.3}$$
$$r_p = r_{p0} + \alpha^2 r_{p1} + \alpha^4 r_{p2} + \cdots \tag{3.4}$$

where $r_p = \frac{\bar{r}_p}{\bar{R}_0}$ is the non – dimensional radius of the plug core.

Using equations (3.1) & (3.3) in equation (2.10), we get

$$\frac{\partial v_{c0}}{\partial t} = \frac{1}{r}\frac{\partial}{\partial r}(r\tau_{c1}) \tag{3.5}$$

$$\frac{\partial}{\partial r}(r\tau_{c0}) = 2r\varphi \tag{3.6}$$

Substituting equations (3.1) & (3.3) in equation (2.11), we have

$$-\frac{\partial v_{c0}}{\partial r} = \tau_{c0} + \tau_y - 2\tau_y^{1/2}.\tau_{c0}^{1/2} \tag{3.7}$$

$$-\frac{\partial v_{c1}}{\partial r} = \tau_{c1}\left[1 - \left(\frac{\tau_y}{\tau_{c0}}\right)^{1/2}\right] \tag{3.8}$$

Using equation (3.1), the boundary conditions (2.13) reduce to

$$\left.\begin{matrix} v_{c0} = v_s \\ v_{c1} = 0 \end{matrix}\right\} \quad \text{at } r = R \tag{3.9}$$

where $R = R(z)$

Integrating equation (3.6) and using condition (2.13), we get

$$\tau_{c0} = r\varphi \tag{3.10}$$

Using equation (3.10), equation (3.7) on integration yields

$$v_{c0} = \frac{1}{2}\varphi(R^2 - r^2) - \frac{4}{3}\tau_y^{1/2}\varphi^{1/2}\left(R^{3/2} - r^{3/2}\right) + \tau_y(R - r) + v_s \tag{3.11}$$

The expression for v_{p0} is obtained by putting $r = r_{p0}$ in equation (3.11) given as

$$v_{p0} = \frac{1}{2}\varphi\left(R^2 - r_{p0}^2\right) - \frac{4}{3}\tau_y^{1/2}\varphi^{1/2}\left(R^{3/2} - r_{p0}^{3/2}\right) + \tau_y\left(R - r_{p0}\right) + v_s \tag{3.12}$$

Integrating equation (3.5) using equation (3.11) and (2.13), we get

$$\tau_{c1} = \frac{1}{2}\varphi'\left(\frac{1}{2}R^2 r - \frac{1}{4}r^3\right) - \frac{2}{3}\tau_y^{1/2}\varphi'\varphi^{-1/2}\left(\frac{1}{2}R^{3/2}r - \frac{2}{7}r^{5/2}\right) \tag{3.13}$$

where $\varphi' = \frac{\partial \varphi}{\partial t}$

Applying equations (3.10) and (3.13) in equation (3.8) and then integrating we obtain

$$v_{c1} = \frac{1}{2}\varphi'\left(\frac{3}{16}R^4 - \frac{1}{4}R^2r^2 + \frac{1}{16}r^4\right) - \frac{2}{3}\tau_y^{1/2}\varphi'\varphi^{-1/2}\left(\frac{33}{196}R^{7/2} - \frac{1}{4}R^{3/2}r^2 + \frac{4}{49}r^{7/2}\right) - \frac{1}{2}\tau_y^{1/2}\varphi'\varphi^{-1/2}\left(\frac{11}{42}R^{7/2} - \frac{1}{3}R^2r^{3/2} + \frac{1}{14}r^{7/2}\right) + \frac{2}{3}\tau_y\varphi'\varphi^{-1}\left(\frac{5}{21}R^3 - \frac{1}{3}R^{3/2}r^{3/2} + \frac{2}{21}r^3\right) \tag{3.14}$$

Substitution of $r = r_{p1}$ in equation (3.14) yields the expression for v_{p1} given as

$$v_{p1} = \frac{1}{2}\varphi'\left(\frac{3}{16}R^4 - \frac{1}{4}R^2r_{p1}^2 + \frac{1}{16}r_{p1}^4\right) - \frac{2}{3}\tau_y^{1/2}\varphi'\varphi^{-1/2}\left(\frac{33}{196}R^{7/2} - \frac{1}{4}R^{3/2}r_{p1}^2 + \frac{4}{49}r_{p1}^{7/2}\right) - \frac{1}{2}\tau_y^{1/2}\varphi'\varphi^{-1/2}\left(\frac{11}{42}R^{7/2} - \frac{1}{3}R^2r_{p1}^{3/2} + \frac{1}{14}r_{p1}^{7/2}\right) + \frac{2}{3}\tau_y\varphi'\varphi^{-1}\left(\frac{5}{21}R^3 - \frac{1}{3}R^{3/2}r_{p1}^{3/2} + \frac{2}{21}r_{p1}^3\right) \tag{3.15}$$

Thus the total axial velocity distribution for the region $r_p \le r \le R(z)$ is

$$v_c = \frac{1}{2}\varphi(R^2 - r^2) - \frac{4}{3}\tau_y^{1/2}\varphi^{1/2}\left(R^{3/2} - r^{3/2}\right) + \tau_y(R - r) + v_s + \alpha^2\left[\frac{1}{2}\varphi'\left(\frac{3}{16}R^4 - \frac{1}{4}R^2r^2 + \frac{1}{16}r^4\right) - \frac{2}{3}\tau_y^{1/2}\varphi'\varphi^{-1/2}\left(\frac{33}{196}R^{7/2} - \frac{1}{4}R^{3/2}r^2 + \frac{4}{49}r^{7/2}\right) - \frac{1}{2}\tau_y^{1/2}\varphi'\varphi^{-1/2}\left(\frac{11}{42}R^{7/2} - \frac{1}{3}R^2r^{3/2} + \frac{1}{14}r^{7/2}\right) + \frac{2}{3}\tau_y\varphi'\varphi^{-1}\left(\frac{5}{21}R^3 - \frac{1}{3}R^{3/2}r^{3/2} + \frac{2}{21}r^3\right)\right] \tag{3.16}$$

The plug flow velocity distribution for the region $0 \le r \le r_p$ is

$$v_p = \frac{1}{2}\varphi\left(R^2 - r_{p0}^2\right) - \frac{4}{3}\tau_y^{1/2}\varphi^{1/2}\left(R^{3/2} - r_{p0}^{3/2}\right) + \tau_y\left(R - r_{p0}\right) + v_s + \alpha^2\left[\frac{1}{2}\varphi'\left(\frac{3}{16}R^4 - \frac{1}{4}R^2 r_{p1}^2 + \frac{1}{16}r_{p1}^4\right) - \frac{2}{3}\tau_y^{1/2}\varphi'\varphi^{-1/2}\left(\frac{33}{196}R^{7/2} - \frac{1}{4}R^{3/2}r_{p1}^2 + \frac{4}{49}r_{p1}^{7/2}\right) - \frac{1}{2}\tau_y^{1/2}\varphi'\varphi^{-1/2}\left(\frac{11}{42}R^{7/2} - \frac{1}{3}R^2 r_{p1}^{3/2} + \frac{1}{14}r_{p1}^{7/2}\right) + \frac{2}{3}\tau_y\varphi'\varphi^{-1}\left(\frac{5}{21}R^3 - \frac{1}{3}R^{3/2}r_{p1}^{3/2} + \frac{2}{21}r_{p1}^3\right)\right] \quad (3.17)$$

The shear stress τ_c is given as

$$\tau_c = r\varphi + \alpha^2\left[\frac{1}{2}\varphi'\left(\frac{1}{2}R^2 r - \frac{1}{4}r^3\right) - \frac{2}{3}\tau_y^{1/2}\varphi'\varphi^{-1/2}\left(\frac{1}{2}R^{3/2}r - \frac{2}{7}r^{5/2}\right)\right] \quad (3.18)$$

The wall shear stress τ_R is obtained as

$$\tau_R = R\varphi + \frac{1}{8}\alpha^2\varphi' R^3 - \frac{1}{7}\alpha^2\tau_y^{1/2}\varphi'\varphi^{-1/2}R^{5/2} \quad (3.19)$$

The non – dimensional volumetric flow rate for the region $0 \le r \le R(z)$ is defined as

$$Q(z,t) = 4\int_0^R r v_c\, dr$$

where $Q(z,t) = \frac{\bar{Q}(\bar{z},\bar{t})}{\pi\bar{p}_0\bar{R}_0^4/8\bar{k}_c}$; $\bar{Q}(\bar{z},\bar{t})$ being the dimensional volumetric flow rate.

Hence

$$Q = 2R^2 v_s + \frac{2}{3}\tau_y R^3 + \frac{1}{2}R^4\left(\varphi + \frac{1}{6}\alpha^2\varphi' R^2 - \frac{15}{77}\alpha^2\tau_y^{1/2}\varphi'\varphi^{-1/2}R^{3/2}\right) - \frac{8}{7}\tau_y^{1/2}R^{7/2}\left(\varphi^{1/2} + \frac{15}{176}\alpha^2\varphi'\varphi^{-1/2}R^2 - \frac{1}{10}\alpha^2\tau_y^{1/2}\varphi'\varphi^{-1}R^{3/2}\right) \quad (3.20)$$

RESULTS AND DISCUSSION

The velocity profile for the axial velocity in the non – plug flow area has been obtained by equation (3.16). The graphical analysis of the results thus obtained are presented in Figs. 1(a) and 1(b).

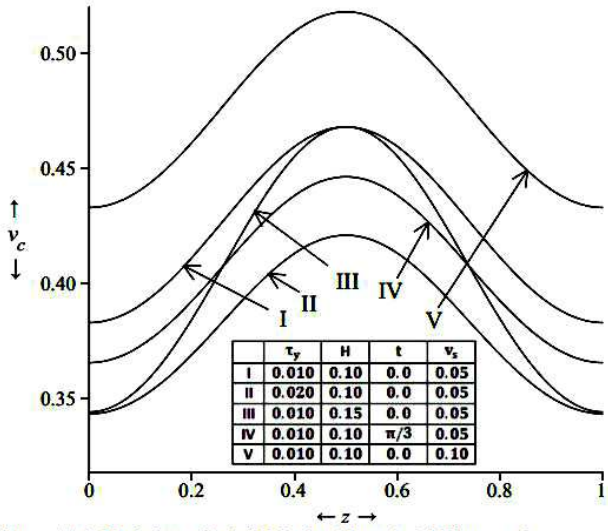

Figure 1 (a): Variation of Axial Velocity Along Axial Distance for Different Values of the Time *t*, Stenosis Height *H*, Yield Stress τ_y and Slip Velocity v_s with Some Fixed Values $e = 0.1$ and $\alpha = 0.1$.

Figure 1(a) describes the variations of the axial velocity versus axial distance for the different values of time t, stenosis height H, yield stress τ_y and slip velocity v_s taking fixed values $e = 0.1$ and $\alpha = 0.1$. The profile shows a natural pattern of fluid flow in a circular duct. There is an increase in velocity with the pulse while slip velocity increases the axial velocity of the fluid. It is found that the axial velocity decreases along the axial distance when time, yield stress and stenosis height increase.

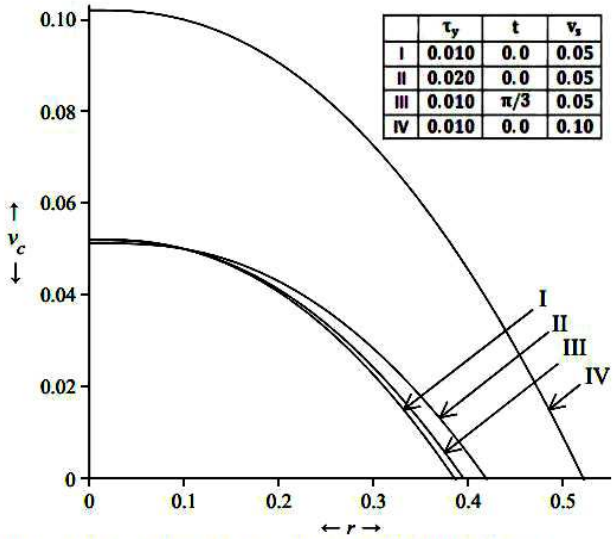

Figure 1 (b): Variation of Axial Velocity Along Radial Distance for Different Values of the Time t, Yield Stress τ and Slip Velocity v_s with Some Fixed Values $e = 0.1$ and $\alpha = 0.1$

Figure 1(b) shows the variations of the axial velocity along radial distance for the various values of time t, yield stress τ_y and slip velocity v_s with some fixed values $e = 0.1$ and $\alpha = 0.1$. It is clear that the axial velocity slows down along the radial distance. Also the axial velocity increases when the time, yield stress and slip velocity increase. A similar graph is obtained showing the increments in the axial velocity with the increase in yield stress.

The graphical analysis of the axial velocity for the plug flow area obtained through equation (3.17) has been described through Figs. 2(a) and 2(b).

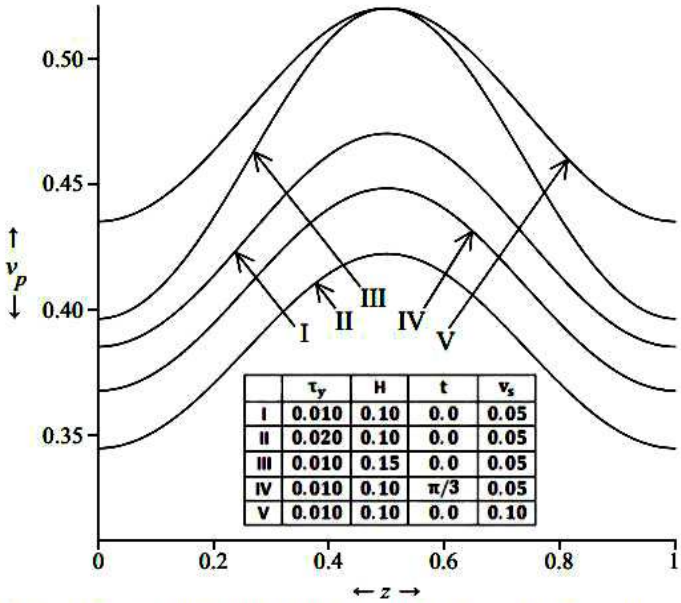

Figure 2 (a): Variation of Plug Flow Velocity Along Axial Distance for Different Values of the Time t, Stenosis Height H, Yield Stress τ_y and Slip Velocity v_s with Some Fixed Values $e = 0.1$ and $\alpha = 0.1$.

Figure 2(a) gives the variations in plug flow velocity along axial distance for the various values of time t, stenosis height H, yield stress τ_y and slip velocity v_s with some fixed values $e = 0.1$ and $\alpha = 0.1$. It shows that the plug flow velocity increases with the increase in axial distance, the stenosis height or slip velocity while it increases with the pulse. Also the plug flow velocity decreases as the yield stress and time increase.

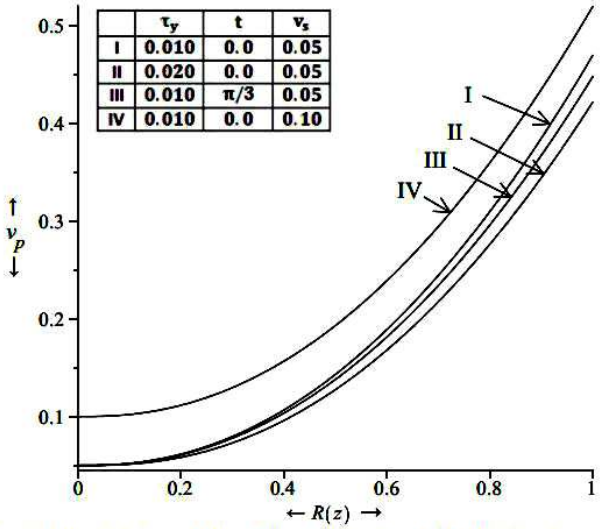

Figure 2 (b): Variation of Plug Flow Velocity Along Radial Distance for Different Values of the Time t, Yield Stress τ_y and Slip Velocity v_s with Some Fixed Values $e = 0.1$ and $\alpha = 0.1$

Figure 2(b) explains the changes in plug flow velocity versus radial distance for the different values of time t, yield stress τ_y and slip velocity v_s with some fixed values $e = 0.1$ and $\alpha = 0.1$. The graph shows that the plug flow velocity increases with increase in the radial distance and slip velocity but it decreases as the time and yield stress increase.

.

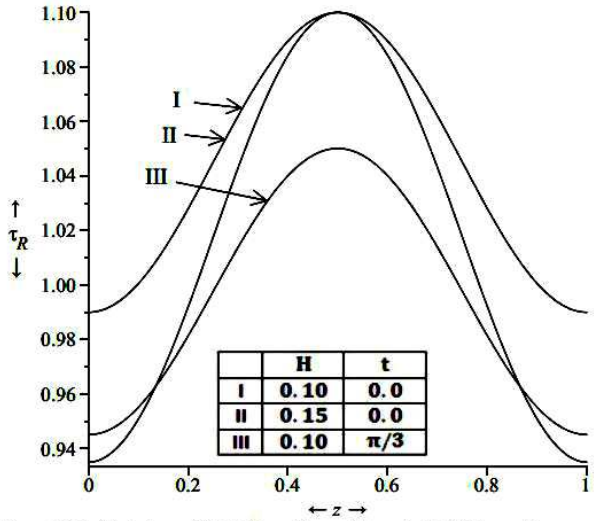

Figure 3 (a): Variation of Wall Shear Stress Along Axial Distance for Different Values of the Time t and Stenosis Height H with Some Fixed Values $e = 0.1$, $\tau_y = 0.010$ and $\alpha = 0.1$.

Figure 3(a) shows the changes in the wall shear stress derived through equation (3.19) along the axial distance for the different values of time t and the stenosis height H with some fixed values $e = 0.1, \tau_y = 0.010$ and $\alpha = 0.1$. It describes that the wall shear stress shows a wave-like variations along the axial distance and it decreases when time and stenosis height increase.

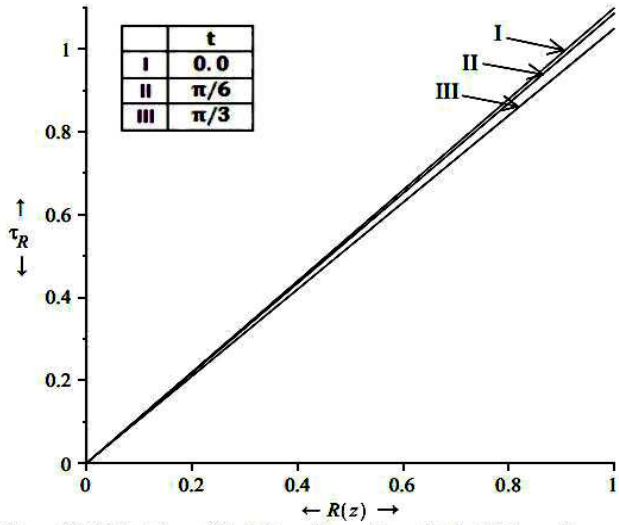

Figure 3 (b): Variation of Wall Shear Stress Along Radial Distance for Different Values of the Time t with Some Fixed Values $e = 0.1$, $\tau_y = 0.010$ and $\alpha = 0.1$

Figure 3(b) gives the variations of the wall shear stress along the radial distance for the different values of time t with some fixed values $e = 0.1, \tau_y = 0.010$ and $\alpha = 0.1$. It is observed that the wall shear stress increases along the radial distance but it decreases when the time increases.

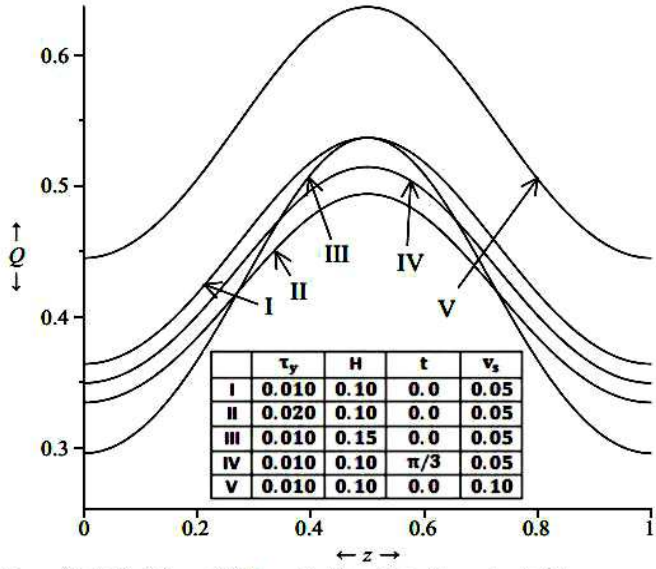

Figure 4 (a): Variation of Volumetric Flow Rate Along the Axial Distance for Different Values of the Time t, Stenosis Height and Slip Velocity v_s with Some Fixed Values $e = 0.1$ and $\alpha = 0.1$.

Figure 4(a) shows the variations of the volumetric flow rate obtained in equation (3.20) versus the axial distance for the different values of time t, stenosis height H, yield stress τ_y and slip velocity v_s taking fixed values $e = 0.1$ and $\alpha = 0.1$. It is observed that the volumetric flow rate fluctuates along the axial distance. The flow rate decreases with increase in time, yield stress or stenosis height but it increases when the slip velocity increases.

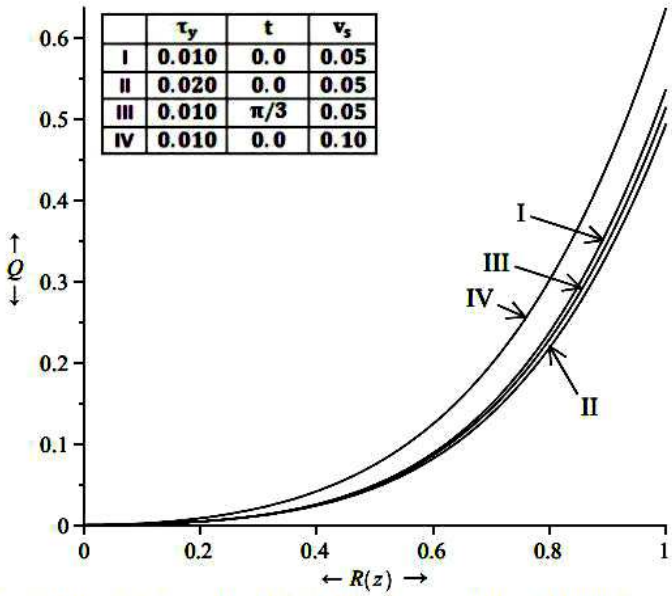

Figure 4 (b): Variation of Volumetric Flow Rate Along Radial Distance for Different Values of the Time *t*, Yield Stress τ_y and Slip Velocity v_s with Some Fixed Values $e = 0.1$ and $\alpha = 0.1$.

Figure 4(b) shows the variations of the volumetric flow rate along the radial distance for the different values of time t, stenosis height H, yield stress τ_y and slip velocity v_s with some fixed values $e = 0.1$ and $\alpha = 0.1$. The graph shows that the volumetric flow rate increases when the radial distance or slip velocity increases. Also it decreases when the time or yield stress increases.

CONCLUSION

In the present model where the Casson fluid is considered as a blood, the Womersley parameter α is taken less than one which is suitable for the small blood vessels like coronary arteries. The non – dimensional yield stress τ_y is taken from 0.01 to 0.03 for a normal state. The flow amplitude "e" is also taken less than one which is reasonable for physiological conditions in normal blood flow. Through the graphical analysis it is observed that the volumetric flow rate and the axial velocity in both plug flow and non – plug flow regions increase with pulse and slip velocity along axial distance but they decrease when time or yield stress increases. The axial velocity in non – plug flow region, flow flux and wall shear stress decrease but the plug flow velocity increases with increase in stenosis height. For $t = 0$ the model reduces to steady state situations which is verified by the author's previous work [11]. The wall shear stress decreases along axial distance when time increases. Also the plug flow velocity, wall shear stress and flow flux increase along radial distance and they decrease when yield stress or time increases. Non – plug flow velocity decreases with increase in radial distance but increases when time, yield stress or slip velocity increases.

REFERENCES

[1] Burton AC, *Physiology and Biophysics of Circulation*, **1966**, Year Book Medical Publisher, Chicago, II.
[2] Young DF, *J. Manuf. Sci. Eng.*, **1968**, 90(2): 248 – 254.
[3] Chaturani P and Samy RP, *Biorheology*, **1986**, Vol. 23 (1986): 499 – 511.
[4] Chakravarty S and Mandal PK, *Mathematical and Computer Modelling*, **1994**, Vol. 19, No. 1: 59 – 70.
[5] Mernone AV and Mazumdar JN, *Mathematical and Computer Modelling*, **2002**, Vol. 35: 895 – 912.
[6] Jung H, Choi JW and Park CG, *Korea-Australia Rheology Journal*, **2004**, Vol. 16, No. 2: 101 – 108.
[7] Pralhad RN and Schultz DH, *Mathematical Biosciences*, **2004**, Vol. 190: 203 – 220.
[8] Volokh KY, *Acta Biomaterialia*, **2006**, Vol. 2: 493 – 504.
[9] Ishikawa T, Kawabata N and Imai Y, *J. Biomechl. Sc. Engg.*, **2007**,Vol. 2, No. 1: 12 – 22.
[10] Siddiqui SU, Verma NK and Gupta RS, *E – Journal of Sc. Tech.*, **2010**, Vol. 4, No. 5: 49 – 66.
[11]Gaur M and Gupta MK, *British J. Math. Comp. Sc.*, **2014**, Vol. 4(11): 1629 – 1641.

[12] Gur M and Gupta MK, *Int. J. Sci. Engg. Res.*, **2014**, Vol. 5, Issue 2: 753 – 758.
[13]Gaur M and Gupta MK, *IJIAS*, **2014**, Vol. 8, No. 1: 394 – 407.
[14] Gaur M and Gupta MK, *Adv. Appl. Sci. Res.*, **2014**, 5(5):249 – 259.